

## Follistatin is essential for normal postnatal development and function of mouse oviduct and uterus

S. J. Holdsworth-Carson<sup>A</sup>, R. G. Craythorn<sup>B</sup>, W. R. Winnall<sup>C</sup>, K. Dhaliwal<sup>B</sup>,  
R. Genovese<sup>B</sup>, C. J. Nowell<sup>D</sup>, P. A. W. Rogers<sup>A</sup>, D. M. de Kretser<sup>B</sup>,  
M. P. Hedger<sup>B</sup> and J. E. Girling<sup>A,B,E</sup>

<sup>A</sup>University of Melbourne Department of Obstetrics and Gynaecology, Royal Women's Hospital, Parkville, Vic. 3052, Australia.

<sup>B</sup>Monash Institute of Medical Research, Monash University, Clayton, Vic. 3168, Australia.

<sup>C</sup>Department of Microbiology and Immunology, University of Melbourne, Parkville, Vic. 3010, Australia.

<sup>D</sup>Ludwig Institute for Cancer Research, Melbourne – Parkville Branch, Vic. 3052, Australia.

<sup>E</sup>Corresponding author. Email: jgirling@unimelb.edu.au

**Abstract.** Female mice lacking the follistatin gene but expressing a human follistatin-315 transgene (tghFST315) have reproductive abnormalities (reduced follicles, no corpora lutea and ovarian–uterine inflammation). We hypothesised that the absence of follistatin-288 causes the abnormal reproductive tract via both developmental abnormalities and abnormal ovarian activity. We characterised the morphology of oviducts and uteri in wild type (WT), tghFST315 and follistatin-knockout mice expressing human follistatin-288 (tghFST288). The oviducts and uteri were examined in postnatal Day-0 and adult mice (WT and tghFST315 only) using histology and immunohistochemistry. Adult WT and tghFST315 mice were ovariectomised and treated with vehicle, oestradiol-17 $\beta$  (100 ng injection, dissection 24 h later) or progesterone (1 mg  $\times$  three daily injections, dissection 24 h later). No differences were observed in the oviducts or uteri at birth, but abnormalities developed by adulthood. Oviducts of tghFST315 mice failed to coil, the myometrium was disorganised, endometrial gland number was reduced and oviducts and uteri contained abundant leukocytes. After ovariectomy, tghFST315 mice had altered uterine cell proliferation, and inflammation was maintained and exacerbated by oestrogen. These studies show that follistatin is crucial to postnatal oviductal–uterine development and function. Further studies differentiating the role of ovarian versus oviductal–uterine follistatin in reproductive tract function at different developmental stages are warranted.

**Additional keywords:** activin A, inflammation, Müllerian duct, myometrium, oestrogen.

Received 4 November 2013, accepted 9 February 2014, published online 17 March 2014

### Introduction

Follistatin (FST) is a monomeric glycoprotein best known for its ability to bind with and neutralise activin A, activin B and some other members of the transforming growth factor  $\beta$  (TGFB) family (including myostatin, the bone morphogenetic proteins-2, -4 and -7, and TGFB3; reviewed by Patel 1998; de Kretser *et al.* 2012). FST is postulated to have key regulatory roles in the development and function of the female reproductive tract (used in this paper to refer to the oviduct and uterus), which matures from the Müllerian duct forming the oviduct, uterus, cervix and anterior vagina. In mouse embryos, the urogenital septum, developing pelvis and gonads are major sites for *Fst* and *activin A* mRNA expression (Day 12 post coitus), where they influence the development of the Müllerian duct (Feijen *et al.* 1994; Hayashi *et al.* 2003; Yao *et al.* 2004). FST can modulate ovarian function by decreasing follicle stimulating hormone (FSH) and

thus influencing follicle and corpus luteum development (reviewed by Knight *et al.* 2012). Considerably less is known about the interactions of activin A and FST within the human uterus and fallopian tube, although these proteins are known to have key roles in the process of decidualisation and the establishment of pregnancy (Petraglia *et al.* 1994; Jones *et al.* 2002a, 2002b; Tierney and Giudice 2004; Refaat and Ledger 2011). Furthermore, *Fst* isoform expression changes throughout the oestrous cycle in rats (Mercado *et al.* 1993) and is increased in the uteri of mice during early pregnancy (Craythorn *et al.* 2012). This study will focus specifically on a role for FST within the developing and adult mouse oviduct and uterus.

There are two major isoforms of FST, FST288 and FST315, both of which are products of a single gene. Both isoforms inhibit FSH secretion by binding with high affinity to activin A, thereby preventing activin from binding to its receptor

(Nakamura *et al.* 1990). FST315 is the main circulating protein and, while FST288 also circulates, its major role is in the interaction with activin at cell surfaces since it is bound to heparin sulfate proteoglycans, facilitating the degradation of activin via a lysosomal pathway (Hashimoto *et al.* 1997). Following FST315–activin complex formation, the complex is capable of binding to the cell surface and activin degradation ensues (Lerch *et al.* 2007). A third isoform also exists, FST303, which is derived from proteolytic cleavage of FST315 and has weaker cell-surface binding properties compared with FST288 (Sugino *et al.* 1993).

Various transgenic mouse models have been developed as tools to study the developmental and functional roles of FST (Matzuk *et al.* 1995; Guo *et al.* 1998; Wankell *et al.* 2001; Jorgez *et al.* 2004; Lin *et al.* 2008; Kimura *et al.* 2010). However, complete deletion of *Fst* resulted in death shortly after birth (Matzuk *et al.* 1995) due to respiratory failure associated with thickened alveolar walls (Lin *et al.* 2008), therefore preventing examination of the role of FST in adult mice. While other tissue-specific models support a role for FST in normal reproduction, they do not help to distinguish the role of FST variants (Guo *et al.* 1998; Jorgez *et al.* 2004). The mouse models used in the present study were produced by creating transgenic mice expressing either human FST288 or FST315 and these mice were crossed with heterozygous *Fst*-null mice (FSTKO). Consequently, mice were available that expressed either FST288 or FST315 in the absence of mouse FST, enabling the assessment of the distinct roles of each human FST isoform (Lin *et al.* 2008). Similar to FSTKO, transgenic mice expressing only human FST288 (tghFST288) died shortly after birth (Matzuk *et al.* 1995; Lin *et al.* 2008). Insertion of the human FST315 (tghFST315) isoform on the FSTKO background prevented the development of the abnormal lung phenotype that caused respiratory failure shortly after birth and these mice survived until adulthood (Lin *et al.* 2008). However, tghFST315 mice have abnormal phenotypic characteristics, including a period of temporary growth retardation (between 15 and 30 days) with subsequent recovery, impaired tail growth and female infertility (Lin *et al.* 2008), which is investigated in greater detail in this paper.

Female tghFST315 mice are infertile, exhibit persistent oestrus associated with the inability to form corpora lutea, have shortened uterine horns and vaginas and overt uterine inflammation (Lin *et al.* 2008). The present study used these transgenic mice as tools to explore the importance of follistatin in oviductal and uterine development (embryonic and postnatal) and function. We aimed to determine whether the reproductive tract (oviduct and uterus) abnormalities in tghFST315 mice reflect deviations in normal development *in utero* (Müllerian duct formation) or the response to abnormal ovarian function and steroid hormone production by adult mice. We hypothesised that the reproductive tract abnormalities would reflect both developmental abnormalities and abnormal ovarian activity.

## Materials and methods

### Animals

For Studies 1 and 3, we used FSTKO, tghFST288 and tghFST315 mice on a C57/129/FVB background. Generation of

FSTKO and transgenic tghFST288 and tghFST315 mice (with the PAC-FS construct) has been described previously (Matzuk *et al.* 1995; Lin *et al.* 2008). Briefly, the PAC-FS vector contained the human *FST* locus including ~45 kb upstream and downstream sequences and was therefore expressed under the control of its endogenous human promoter (Lin *et al.* 2008). The tghFST288 and tghFST315 mice expressed no endogenous mouse *Fst* and carried only the engineered human FST288 or FST315-specific constructs, respectively. Further, it should be noted that tghFST315 mice are also a FST-deficient model; the expression of the human *FST* transgene in adult tghFST315 mice is reduced relative to mouse FST315 production in wild type (WT) animals (Lin *et al.* 2008). WT control mice were derived from the same colony while breeding the transgenic animals. For Study 2, C57/CBA WT mice were used to examine basal expression of *Fst* and related genes in the reproductive tract throughout oestrus and following superovulation (see Supplementary Material). Animals were housed in controlled environmental conditions (20°C, 12 h light:dark cycles and with food and water available *ad libitum*). Animal experiments were approved by the Monash Medical Centre Committee A.

### Study 1: examination of FST transgenic oviducts and uteri

In order to determine whether abnormalities develop during embryonic development or postnatally, oviducts and uteri of *FST* transgenic mice were compared with WT animals on the day of birth (designated as postnatal Day 0, PND0; WT  $n = 3$ , FSTKO  $n = 3$ , tghFST288  $n = 3$  and tghFST315  $n = 3$ ) and as 8-wk adults (WT  $n = 3$  and tghFST315  $n = 3$ ; note that FSTKO and tghFST288 mice do not survive to adulthood). Prior to culling, vaginal smears were performed on mice to establish oestrous cycle stage (Marcondes *et al.* 2002). Gross appearance of the internal reproductive tract was recorded. Reproductive tract tissues were dissected and immediately fixed in 10% buffered formalin for 4 h. Longitudinal (PND0) and cross (adult mice) sections were subsequently examined using haematoxylin and eosin (H&E) staining and immunohistochemistry with antibodies directed against leukocytes (CD45), endothelial cells (CD31) and smooth muscle cells ( $\alpha$  smooth muscle actin ( $\alpha$ SMA); Table 1).

### Study 2: expression of FST in WT and tghFST315 uteri

The experiments in this study were undertaken to provide baseline information about the expression of FST and related molecules in the reproductive tract of WT mice before comparing expression in tghFST315 versus WT mice. We examined the basal expression of *Fst315* and *Fst288* and related genes (*Inhba* and *Inha*) along the length of the mouse reproductive tract and through the oestrous cycle (uterus only, age 6–8 wks). We also examined mRNA expression in the uterus of pre-pubertal (5-wk) WT mice following induction of a cohort of follicles and subsequent formation of corpora lutea using a superovulation protocol; superovulation was induced in these mice to magnify the effects of endogenous hormones on the ovary and uterus (see Supplementary Material for details). We subsequently examined the expression of *Fst* and related

Table 1. Immunohistochemistry protocols

Primary antibody	Antigen retrieval	Peroxidase quench	Antibody concentration	Incubation	Secondary antibody	Detection
Rat anti-mouse CD45 (BD Pharmingen, San Jose, CA, USA) or rat IgG <sub>2b</sub> negative control (BD Pharmingen)	Citrate buffer, pH6.0, 15 min at 100°C	3% H <sub>2</sub> O <sub>2</sub> , 10 min at RT	10 µg mL <sup>-1</sup>	1 h at RT	Biotinylated goat anti-rat IgG (1 : 200; Millipore, Billerica, MA, USA), Vectastain ABC Kit (Vector Laboratories)	DAB
Rat anti-mouse CD31 (BD Pharmingen) or rat IgG <sub>2b</sub> negative control (BD Pharmingen)	0.1% Pepsin, 10 min at 37°C		0.5 µg mL <sup>-1</sup>	2 nights at 4°C	Biotinylated goat anti-rat IgG (1 : 200; Millipore), LSAB+ System-AP (Dako)	Vector blue
Mouse monoclonal αSMA (Dako) or mouse IgG <sub>2a</sub> negative control (Dako)	–	3% H <sub>2</sub> O <sub>2</sub> , 10 min at RT	0.35 µg mL <sup>-1</sup>	Overnight at 4°C	Biotin-SP-conjugated Fab fragment goat anti-mouse IgG (1 : 250; Jackson ImmunoResearch Laboratories), HRP-streptavidin (Dako)	DAB
Sheep monoclonal anti-BrdU (BioDesign International, Saco, ME, USA) or sheep IgG negative control (Sigma-Aldrich)	1.5 M HCl, 15 min at 37°C; 0.1 M borate buffer, 10 min at RT	3% H <sub>2</sub> O <sub>2</sub> , 10 min at RT	8 µg mL <sup>-1</sup>	1 h at RT	Biotinylated donkey anti-sheep IgG (1 : 200; Jackson ImmunoResearch Laboratories), HRP-streptavidin (Dako)	DAB

molecules in the uterus of tghFST315 mice relative to WT animals as outlined below.

Vaginal smears were performed on adult tghFST315 mice and no evidence of cycling was observed, consistent with earlier observations (Lin *et al.* 2008). Smears from tghFST315 mice showed clumped cornified epithelial cells and were most similar to vaginal smears from WT mice during oestrus (Fig. 4a–b). Thus, tghFST315 mice ( $n = 5$ ) were compared with WT mice at oestrus (11:00am;  $n = 5$ ). Following reproductive tract dissection, tissues were snap frozen in an isopropanol–dry ice slurry and stored at  $-80^{\circ}\text{C}$ . Blood was collected by cardiac puncture. Frozen tissues or blood underwent RNA or protein isolation for quantitative polymerase chain reaction with reverse transcription (qRT-PCR) or radio-immuno assay (RIA) or enzyme-linked immunosorbent assay (ELISA) analyses, respectively.

### Study 3: effect of ovarian hormones on tghFST315 uteri

In this study we examined hormone-treated ovariectomised tghFST315 mice to determine whether their uteri are able to appropriately respond to steroid hormones and to elucidate whether the reproductive tract abnormalities, particularly inflammation, reflect the altered ovarian function and abnormalities independent of the ovary. Weight-matched female WT (6–8 wk, 17–24 g bodyweight) and tghFST315 (8–10 weeks, 17–24 g) mice were ovariectomised to remove the influence of the ovaries on the uterine phenotype. Transgenic mice were slightly older because tghFST315 mice do not demonstrate mating behaviour until  $\sim 8$  wks of age (Lin *et al.* 2008). Following bilateral ovariectomy, mice were left for a minimum of 7 days to recover and to allow for endometrial regression, before one of two steroid hormone protocols commenced (Heryanto and Rogers 2002; Walter *et al.* 2005, 2010; Girling *et al.* 2007). Protocol 1 (short-term oestrogen, E): mice were given a single subcutaneous (s.c.) injection of oestradiol-17 $\beta$  (100 ng in 100 µL peanut oil; Sigma-Aldrich, St Louis, MO, USA) or vehicle (100 µL peanut oil) 8 days post-ovariectomy ( $n = 7-9$  per group). This was followed by an intra-peritoneal (i.p.) injection of BrdU (500 µL of 40 mg kg<sup>-1</sup> bodyweight; Sigma-Aldrich) 20 h later. Day 9 post-ovariectomy (24 h after steroid and 4 h after BrdU), mice were dissected. Protocol 2 (progesterone, P): this regime was designed to mimic the effects of progesterone during early pregnancy. WT and tghFST315 mice ( $n = 7$  per group) received s.c. injections of progesterone (1 mg in 100 µL peanut oil; Sigma-Aldrich) on Days 10, 11 and 12 post-ovariectomy. BrdU injections were administered (as above) 4 h before dissection on Day 13. At the time of dissection, blood and reproductive tract tissues were collected and processed as for Studies 1 and 2. Mouse uteri were used to examine endothelial, epithelial and stromal cell proliferation and CD45 leukocyte distribution.

### Immunohistochemistry (IHC) and image analysis

Fixed tissue was embedded in paraffin and sectioned (3 µm) on 3-amino propyltriethoxy silane- (APES; Sigma-Aldrich) coated slides. The basic morphology of tissues was examined after standard HandE staining. Blood vessels were identified using an antibody against the pan-endothelial cell marker CD31.

Leukocytes were identified with an antibody against CD45 and smooth muscle with an antibody against smooth-muscle actin ( $\alpha$ SMA). See Table 1 for a summary of antibodies and IHC protocols. All paraffin sections were dewaxed and rehydrated before antigen retrieval (except  $\alpha$ SMA, specific details in Table 1) and endogenous peroxidase inactivation (3% (v/v)  $H_2O_2$ ) except CD31. Sections were blocked (10 min at room temperature (RT)) with serum-free protein block (Dako, Glostrup, Denmark). Sections stained for  $\alpha$ SMA had an additional blocking step with unconjugated AffiniPure Fab fragment goat anti-mouse IgG ( $H^+L$ , 0.1 mg mL<sup>-1</sup>; Jackson Immuno-Research Laboratories, West Grove, PA, USA) for 1 h at RT. The primary antibodies or isotype-matched controls were then added as per details in Table 1. This was followed by incubations with secondary antibody (Table 1). CD45 immunostaining was visualised using Vectastain ABC (30 min at RT; Vector Laboratories, Inc., Burlingame, CA, USA) and 3,3'-diaminobenzidine (DAB, 5 min at RT; Sigma-Aldrich). Slides were briefly counterstained with haematoxylin. CD31 staining was detected with the LSAB+ System-AP kit (15 min at RT; Dako), followed by Vector Blue alkaline phosphatase chromagen (15 min at RT; Vector Laboratories).  $\alpha$ SMA and BrdU sections were incubated with horse radish peroxidase (HRP)–streptavidin (10 min for RT; Dako) and visualised with DAB.

Sections were observed and images acquired using a Zeiss Axioskop microscope, AxioCam ICc3 camera and AxioVision software (Carl Zeiss, Jena, Germany). Images from ovariectomy studies were scanned on an Aperio ScanScopeXT (Aperio, Buffalo Grove, IL, USA). For quantitative image analysis,  $n = 6-9$  mice were included per group with  $n = 1-3$  slides counted on average per mouse. The colour deconvolution module in Fiji (image processing package based on ImageJ; Schindelin *et al.* 2012) was used on scanned image files to quantify BrdU and CD45 staining. Positive and negative channels were used in the Cell Scoring application of MetaMorph (Meta Imaging Series 7.7; Molecular Devices, Sunnyvale, CA, USA) to count positive and negative cells (Fig. 7b). Counts were then generated for user-defined tissue layers (endometrium, myometrium, luminal epithelium and glandular epithelium; Fig. 7c). Proliferating BrdU-positive endothelial cells were counted using the Cell Counter plugin in Fiji (ImageJ) and expressed as the number of BrdU-positive cells per vessel profile. Proliferating BrdU-positive luminal and glandular epithelial cells were counted manually and were expressed as a percentage of BrdU-positive cells. Proliferating stromal cells were expressed as BrdU-positive cells mm<sup>-2</sup>. CD45 cell data is represented as a percentage of CD45-positive cells in the region of interest.

#### Quantitative RT-PCR (qRT-PCR)

Messenger RNA was isolated from frozen uterine tissue following homogenisation (Pro200 hand-held homogeniser; PRO Scientific Inc., Oxford, CT, USA or PowerLyzer 24 bench top bead-based homogeniser; MO BIO Laboratories, Inc., Carlsbad, CA, USA) in 1 mL of TRIzol reagent and treatment with Turbo DNase (4U; both from Life Technologies, Carlsbad, CA, USA) according to the manufacturer's instructions. PureLink RNA Mini Kit columns (using TRIzol) were used when limited

**Table 2. Primer sequences**

Gene	Primer sequence
m Fst288 F	5' CTC TCT CTG CGA TGA GCT GTG T 3'
m Fst288 R	5' GGC TCA GGT TTT ACA GGC AGA T 3'
m Fst315 F	5' CTC TCT CTG CGA TGA GCT GTG T 3'
m Fst315 R	5' TCT TCC TCC TCC TCC TCT TCC T 3'
h FST315 F	5' GTC TGT GCC AGT GAC AAT GC 3'
h FST315 R	5' GTC TTC CGA AAT GGA GTT GC 3'
Inhba F	5' TGG AGT GTG ATG GCA AGG TC 3'
Inhba R	5' AGC CAC ACT CCT CCA CAA TC 3'
Inha F	5' TGG GGA GGT CCT AGA CAG AAA GGG C 3'
Inha R	5' GGC TGG TCC TCA CAG GTG GCA C 3'
RNA spike F	5' ACT CAC TAT AGG GCG AAT TGG A 3'
RNA spike R	5' GAG CGG ATA ACA ATT TCA CAC A 3'
18s F	5' GCG GCT TAA TTT GAC TCA ACA C 3'
18s R	5' CGT TCG TTA TCG GAA TTA ACC A 3'

amounts of tissue were available (Life Technologies). Quality and concentration of RNA was determined using a Nanodrop UV spectrophotometer (Thermo Fisher Scientific, Scoresby, Vic., Australia). RNA (1  $\mu$ g) was converted into cDNA using a High-Capacity cDNA Reverse Transcription Kit with RNase inhibitor (Life Technologies). Each cDNA master-mix reaction contained an equal amount of *in vitro*-transcribed RNA spike and a 300-bp region of the T7 promoter region of the pBluescript phagemid (Winnall *et al.* 2009). This spike controls for the efficiency of the cDNA reaction (Craythorn *et al.* 2009; Winnall *et al.* 2009). Following cDNA synthesis, samples were diluted 1 : 10 in nuclease-free sterile water.

Quantitative RT-PCR analysis was performed using FastStart DNA Master SYBR Green I (Roche Applied Sciences, Indianapolis, IN, USA) or Power SYBR Green PCR Master Mix (Life Technologies) and an iQ5 machine (Bio-Rad Laboratories, Hercules, CA, USA) or Applied Biosystems 7500/7500 Fast Real-Time PCR System (Life Technologies). Specific primers for the detection of each gene, mouse *Fst288*, mouse *Fst315*, human *FST315*, mouse *Inhba*, mouse *Inha*, *18s* and RNA spike are described in Table 2. PCR products were run on 1.5% agarose gels and purified using the Wizard SV Gel and PCR Clean-Up kit (Promega, Madison, WI, USA). Primer targets were confirmed by sequencing purified PCR products, which was performed by the Australian Genome Research Facility (Parkville, Vic., Australia). In the qRT-PCR reaction, cDNA (1  $\mu$ L, diluted 1 : 10) was included per 10- $\mu$ L reaction. Sense and antisense primers, at a final concentration of 150 nM, were included per reaction. Amplification and standard curves were performed as previously described (Winnall *et al.* 2011). Messenger RNA from PND0 FSKO mice, ovarian tissue from adult WT mice and human myometrium were included as internal controls. The RNA spike was used to normalise the data (Craythorn *et al.* 2009; Winnall *et al.* 2009) and was detected at the same level in each tissue (data not shown). Utilisation of spike was particularly important for investigations of the oestrous-cycle stage as housekeeping genes, such as *18S*, are influenced by steroid hormones (Craythorn *et al.* 2009). All data were analysed by relative quantification to the RNA spike, using the method described by Pfaffl (2001).

### RIA and ELISA

Frozen tissue was homogenised and protein extracted in phosphate-buffered saline (PBS) with protease inhibitor (1:200) (Calbiochem, San Diego, CA, USA). Total protein concentration ( $\text{mg mL}^{-1}$ ) was determined using the DC Protein Assay (Bio-Rad Laboratories) according to the manufacturer's instructions. Total FST (bound and unbound) protein was measured from uterine homogenates and serum using a discontinuous RIA (O'Connor *et al.* 1999). Activin A ( $\beta$ A subunit) protein was measured using a commercially available sandwich ELISA (Oxford Bio-Innovations, Cherwell, UK) with some modifications (O'Connor *et al.* 1999). Uterine and serum FST and activin concentrations ( $\text{ng mL}^{-1}$ ) were normalised against total protein, and were expressed as ng of FST or activin A per mg of total protein.

### Statistics

Statistical analysis was performed using SPSS (Version 20; SPPS Inc., Armonk, NY, USA). Expression of mRNA and protein from WT animals (cycling and superovulation experiments) and WT versus tghFST315 ovariectomy experiments were compared using one- or two-way ANOVA followed by a post-hoc analysis (Tukey's) when appropriate. Expression of mRNA and protein from WT versus tghFST315 mice (Study 2) was analysed using independent sample *t*-tests. A value of  $P \leq 0.05$  was considered to be significant.

## Results

### Study 1

#### *No abnormalities were noted in the uteri of postnatal Day 0 (PND0) FST transgenic mice*

In this study we examined whether reproductive tract abnormalities occurred during embryonic development or postnatally. There were no overt differences in the uteri of PND0 FSTKO (Fig. 1*b*), tghFST288 (Fig. 1*c*) and tghFST315 (Fig. 1*d*) mice relative to WT mice (Fig. 1*a*). The uteri of WT and transgenic mice were simple tubes lined with epithelial cells (Fig. 1*e-h*). As expected, the endometrium and myometrium of WT and FST transgenic mice were not fully developed by PND0, illustrated by the lack of  $\alpha$ SMA immunostaining (Fig. 1*m-p*). However, segregation of the uterine mesenchymal cells into layers (inner, middle and outer) was apparent (Brody and Cunha 1989). Occasional leukocytes were observed in the uterine mesenchyme at PND0 for WT and transgenic mice (Fig. 1*i-l*, arrows); however, populations of leukocytes were not different between genotypes. While smooth-muscle staining was absent at PND0 in all mice, blood-vessel staining was prominent and did not demonstrate any overt differences between WT and FST transgenic mice (Fig. 1*m-p*).

#### *The oviducts and uteri of adult tghFST315 mice were abnormal*

FSTKO and tghFST288 mice do not survive postnatally (Lin *et al.* 2008) and thus analysis of adult oviducts and uteri was restricted to WT and tghFST315 mice.

Confirming our earlier work (Lin *et al.* 2008), macroscopically, the uteri of adult tghFST315 mice were abnormal

(Fig. 2*b-d*) compared with WT mice (Fig. 2*a*) and demonstrated great variability. Commonly observed deformities of the uteri included oedematous and distended uterine horns with areas of narrowing consistent with fibrosis and scarring. There were also a large number of leukocytes present within the uteri of tghFST315 mice (Fig. 2*e-h*) consistent with our previous study (Lin *et al.* 2008). In tghFST315 mice the CD45-positive cells were observed in the luminal epithelium, myometrium and endometrial stroma (Fig. 2*g-h*). In contrast, in WT uteri this increase was mainly found in the endometrial stroma, to a lesser extent in the myometrium and not in the luminal epithelium (Fig. 2*e-f*). As previously described (Lin *et al.* 2008), the leukocytes in tghFST315 mice were predominately neutrophils characterised by their multi-lobed nuclei.

Abnormalities of the tghFST315 endometrial and myometrial layers were clearly illustrated when  $\alpha$ SMA immunostaining was used (Fig. 2*i-l*). Mature WT mice had distinct circular and longitudinal myometrial muscle layers (Fig. 2*i-j*). On the other hand, the uterine myometrial smooth muscle in tghFST315 mice was highly disorganised, particularly the circular myometrial layer, which varied in thickness and had a reduced muscle-fibre density (Fig. 2*k-l*). Blood vessels identified by CD31 immunostaining were comparable between WT and tghFST315 uteri (Fig. 2*i-l*). We also observed a reduction in the number of endometrial glands in tghFST315 mice compared with WT (Fig. 2*e-h*); this is discussed further in Study 3.

The oviduct of tghFST315 adult mice (Fig. 3*b*) lacked coiling compared with WT mice (Fig. 3*a*). As in the uterus, the oviducts of tghFST315 mice had extensive leukocyte infiltration (neutrophils) both in their lumen and walls compared with WT mice (Fig. 3*c-e* and *f-h*). As with the uterus, the pattern of  $\alpha$ SMA was altered in the tghFST315 mice, demonstrating varying degrees of thickness and levels of organisation (Fig. 3*i-k*). The blood vessels in the uterine tubes, as stained by CD31, were similar between oviducts of WT and tghFST315 mice (Fig. 3*i-k*).

### Study 2

#### *Uterine Fst expression was unchanged during the WT oestrous cycle*

Experiments were undertaken to provide baseline information about the expression of *Fst* and related molecules in the reproductive tract of WT mice (see Supplementary Material for detailed results). We subsequently compared expression in tghFST315 versus WT mice. In normal cycling female mice, the expression levels of *Fst288* and *Fst315* mRNA were highest in the ovary relative to other parts of the tract examined (see Fig. S1*a-b*, available as Supplementary Material to this paper). There was no significant change in uterine mRNA expression of *Fst288*, *Fst315* or *Inha* through the oestrous cycle, although there were significant changes in uterine *Inhba* mRNA expression (Fig. S2*a-d*). Total FST protein concentrations were unchanged throughout the oestrous cycle in WT uterine homogenates and sera; however, significant changes were noted in the protein levels of uterine, but not serum, activin A (Fig. S2*e-h*).

*Fst288*, *Fst315*, *Inhba* and *Inha* mRNA were all expressed in pre-pubertal, non-cycling mouse uteri. However, superovulation failed to induce any significant change in uterine mRNA

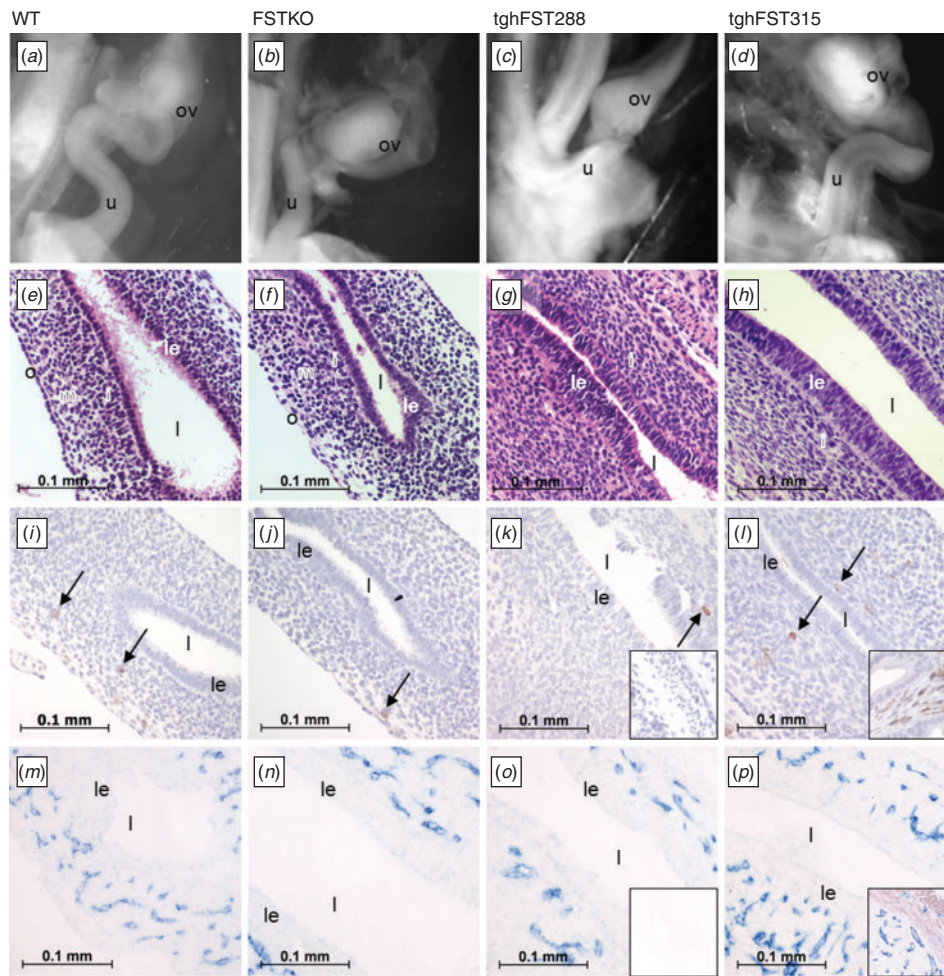


**Fig. 1.** PND0 female FST transgenic mice have normal internal reproductive tracts and histology. Appearance of the internal reproductive tract on PND0 for (a) WT, (b) FSTKO, (c) tghFST288 and (d) tghFST315 mice. Representative micrographs of HandE-stained mouse uteri from (e) WT, (f) FSTKO, (g) tghFST288 and (h) tghFST315 animals. Representative micrographs of CD45 immunostaining from (i) WT, (j) FSTKO, (k) tghFST288 (inset: isotype-matched negative control) and (l) tghFST315 (inset: adult mouse uterus positive control) mouse uteri. CD45-positive cells are indicated by thin black arrows. Representative micrographs of CD31- $\alpha$ SMA double immunostaining from (m) WT, (n) FSTKO, (o) tghFST288 (inset: isotype-matched negative control) and (p) tghFST315 (inset: adult mouse uterus positive control) mouse uteri.  $\alpha$ SMA could not be detected in PND0 uteri, refer to inset (p) where positive brown staining for  $\alpha$ SMA is apparent. Samples sizes were  $n = 3$  per genotype. Scale bar is equal to 0.1 mm. ov, ovary; u, uterine horn; l, lumen; le, lumen epithelium; o, outer mesenchymal layer; m, middle mesenchymal layer; i, inner mesenchymal layer.

expression of *Fst288*, *Fst315*, *Inhba* or *Inha*, uterine and serum expression of activin A protein or serum total FST protein, compared with vehicle-treated mice. In contrast, uterine total FST protein was significantly elevated in both the pregnant mare's serum gonadotropin (PMSG) and PMSG plus human chorionic gonadotrophin (hCG) treatment groups compared with the vehicle group (Fig. S3).

As previously reported (Lin *et al.* 2008), adult tghFST315 mice do not have a normal oestrous cycle and demonstrate persistent oestrus as shown by daily vaginal smear cytology. An example of a daily vaginal smear from a tghFST315 adult mouse shows an abundance of clumped cornified epithelial cells

(Fig. 4b), most similar to those from the oestrous phase of a normal cycling WT mouse (Fig. 4a). Thus, for the following part of Study 2, tghFST315 mice were compared with WT mice at oestrus (11:00am).

#### *Total FST protein was reduced in adult tghFST315 mice compared with WT mice in oestrus*

The tghFST315 mice were engineered to express only the human *FST315* gene (Lin *et al.* 2008). No mouse *Fst288* or *Fst315* mRNA were expressed in tghFST315 mice (*Fst288* WT:  $2.12 \pm 1.27$ , tghFST315:  $0.02 \pm 0.00$  and *Fst315* WT:  $2.23 \pm 1.43$ , tghFST315:  $0.02 \pm 0.00$ ). In contrast, human

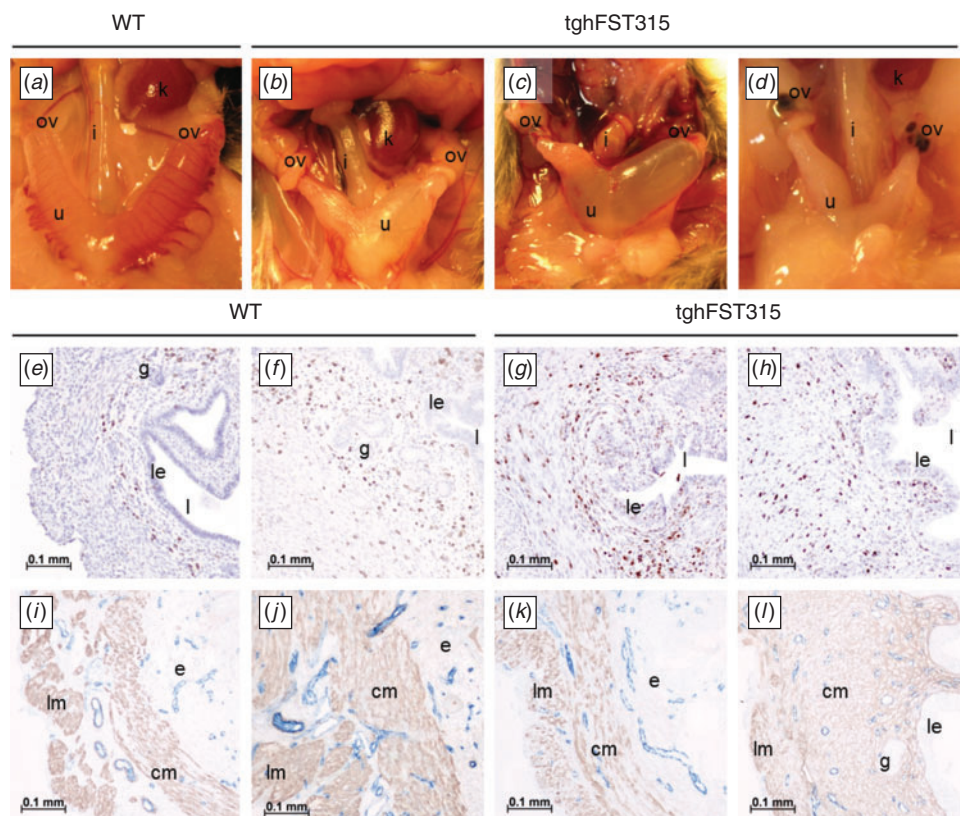


**Fig. 2.** Adult tghFST315 females have abnormal reproductive tracts compared with WT mice. Appearance of the internal reproductive tract of the (a) adult WT (during proestrus) and (b–d) tghFST315 mouse. As previously noted (Lin *et al.* 2008), there is substantial variability in the appearance of the tghFST315 tract, including the ovary. To illustrate the leukocyte infiltrate noted by (Lin *et al.* 2008), we undertook CD45 (brown) immunostaining from (e, f) WT and (g, h) tghFST315 mouse uteri. Note the presence of CD45-positive cells in the lumen epithelium from tghFST315 animals. Representative micrographs of CD31 (blue) and  $\alpha$ SMA (brown) double immunostaining from (i, j) WT and (k, l) tghFST315 mouse uteri. Samples sizes were  $n = 3$  per genotype. Scale bar is equal to 0.1 mm. ov, ovary; i, inferior vena cava; u, uterine horn; k, kidney; l, lumen; le, lumen epithelium; g, glands; cm, circular myometrial layer; lm, longitudinal myometrial layer; e, endometrial stroma.

*FST315* was present in tghFST315 uteri compared with WT (range WT: 0.08–3.64, tghFST315: 2.81–13.60;  $P = 0.056$ ). The human *FST315* primer (Table 2) exhibited a degree of cross-reactivity with the mouse genome, which helps to explain the small level of amplification seen in WT mice.

The mRNA expression of *Inhba* and *Inha* was not different in the uteri of tghFST315 mice compared with WT uteri (Fig. 4c–d). There were no significant differences between activin A protein levels in WT and tghFST315 mouse uteri (Fig. 4e). In contrast, circulating levels of activin A were significantly increased in tghFST315 mice compared with WT animals (tghFST315:  $353.1 \pm 43.0$  pg mL<sup>-1</sup>, WT:  $116.9 \pm 7.9$  pg mL<sup>-1</sup>;  $P = 0.0001$ ; Fig. 4f).

The tghFST315 mice had significantly altered serum and uterine levels of total FST protein; WT mice had 3-fold higher circulating total FST compared with tghFST315 mice (WT:  $5.9 \pm 0.3$  ng mL<sup>-1</sup>, tghFST315:  $2.1 \pm 0.5$  ng mL<sup>-1</sup>;  $P < 0.001$ ; Fig. 4g). In uterine homogenates the concentration of total FST was significantly higher in the WT uteri compared with tghFST315 mice (WT:  $15.2 \pm 2.1$  ng mg<sup>-1</sup> of protein,

tghFST315:  $5.4 \pm 1.4$  ng mg<sup>-1</sup> of protein;  $P = 0.005$ ; Fig. 4h). This difference in total FST levels may reflect the absence of FST288 in the tghFST315 mouse.

### Study 3

#### *Uterine cell proliferation is altered in tghFST315 mice following ovariectomy*

In this experiment, adult WT and tghFST315 mice were ovariectomised to remove the influence of the tghFST315 ovary on the uterine phenotype. Ovariectomised mice were treated with two different protocols (E or P) with a two-fold purpose; first to determine if tghFST315 uteri can respond like WT uteri to ovarian steroid hormones, and second to evaluate if removal of the ovary alleviates the abnormalities, particularly inflammation, present in tghFST315 uteri.

In ovariectomised adult WT and tghFST315 mice proliferating cells were identified in the myometrial and endometrial stroma, glandular and luminal epithelium and blood vessel endothelium in both WT and tghFST315 mice by their staining

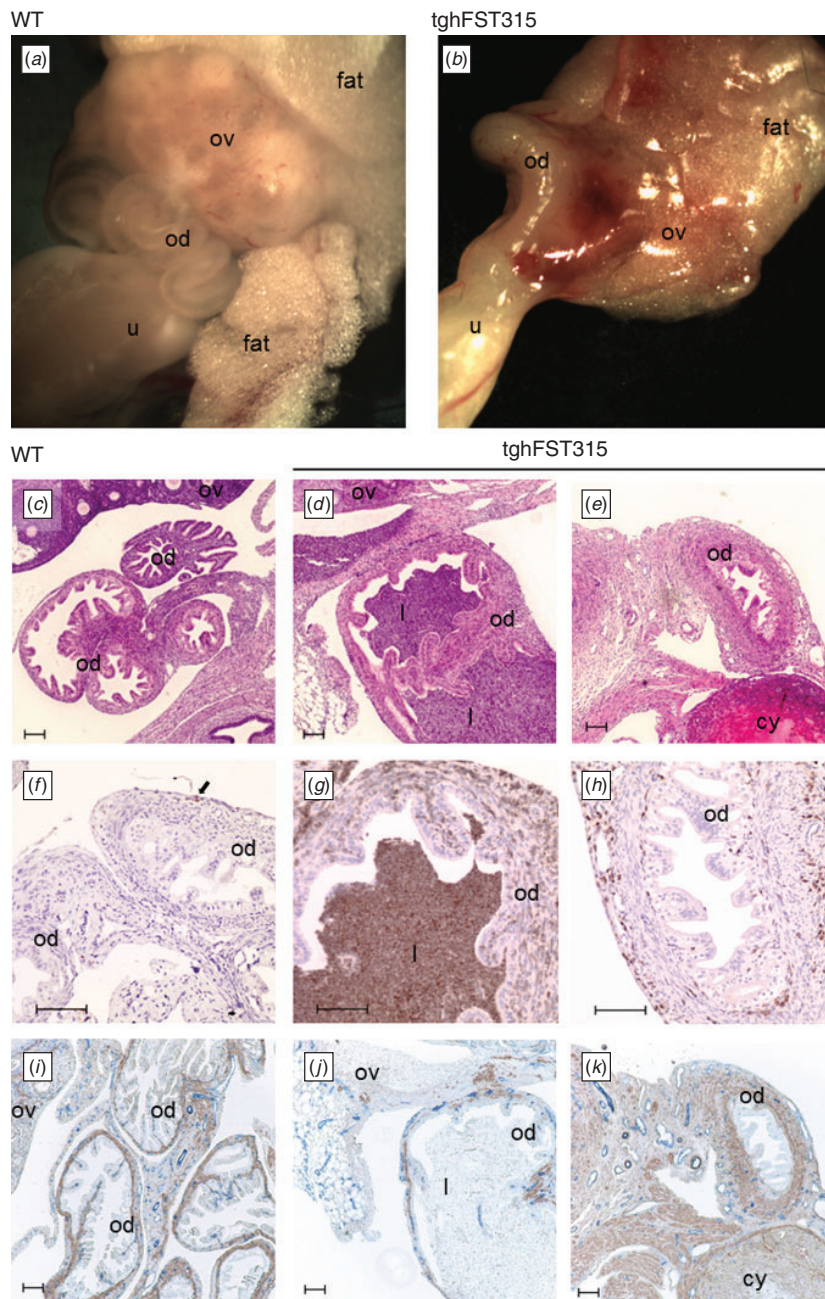


**Fig. 3.** The oviducts of adult tghFST315 mice are malformed. Gross appearance of the oviduct, ovary and adjoining uterine horn of adult (a) WT and (b) tghFST315 mice. Representative micrographs of HandE-stained oviduct sections from (c) WT and (d–e) tghFST315 reproductive tracts. Representative micrographs of CD45-immunostained (f) WT and (g–h) tghFST315 oviducts and CD31 (blue) and  $\alpha$ SMA (brown) double immunostaining from (i) WT and (j–k) tghFST315 oviducts. Samples sizes were  $n = 3$  per genotype. Scale bar is equal to 0.1 mm. *ov*, ovary; *u*, uterine horn; *od*, oviduct; *fat*, fat pad; *l*, leukocytes; *cy*, ovarian cyst.

for BrdU (Fig. 5a–f). Overall tghFST315 mice had a subtle, but significant increase in endometrial stromal cell proliferation relative to WT mice ( $F_{(1,35)} = 7.522$ ,  $P = 0.010$ ; Fig. 6a). In WT and tghFST315 mice, hormone treatments (E or P) increased

endometrial stromal cell proliferation in the endometrium compared with the vehicle group (vehicle:  $124.6 \pm 55.5$  cells  $\text{mm}^{-2}$ , E:  $331.2 \pm 53.2$  cells  $\text{mm}^{-2}$ , P:  $362.6 \pm 55.3$  cells  $\text{mm}^{-2}$ ,  $F_{(2,35)} = 5.488$ ,  $P = 0.008$ ; Fig. 6a).

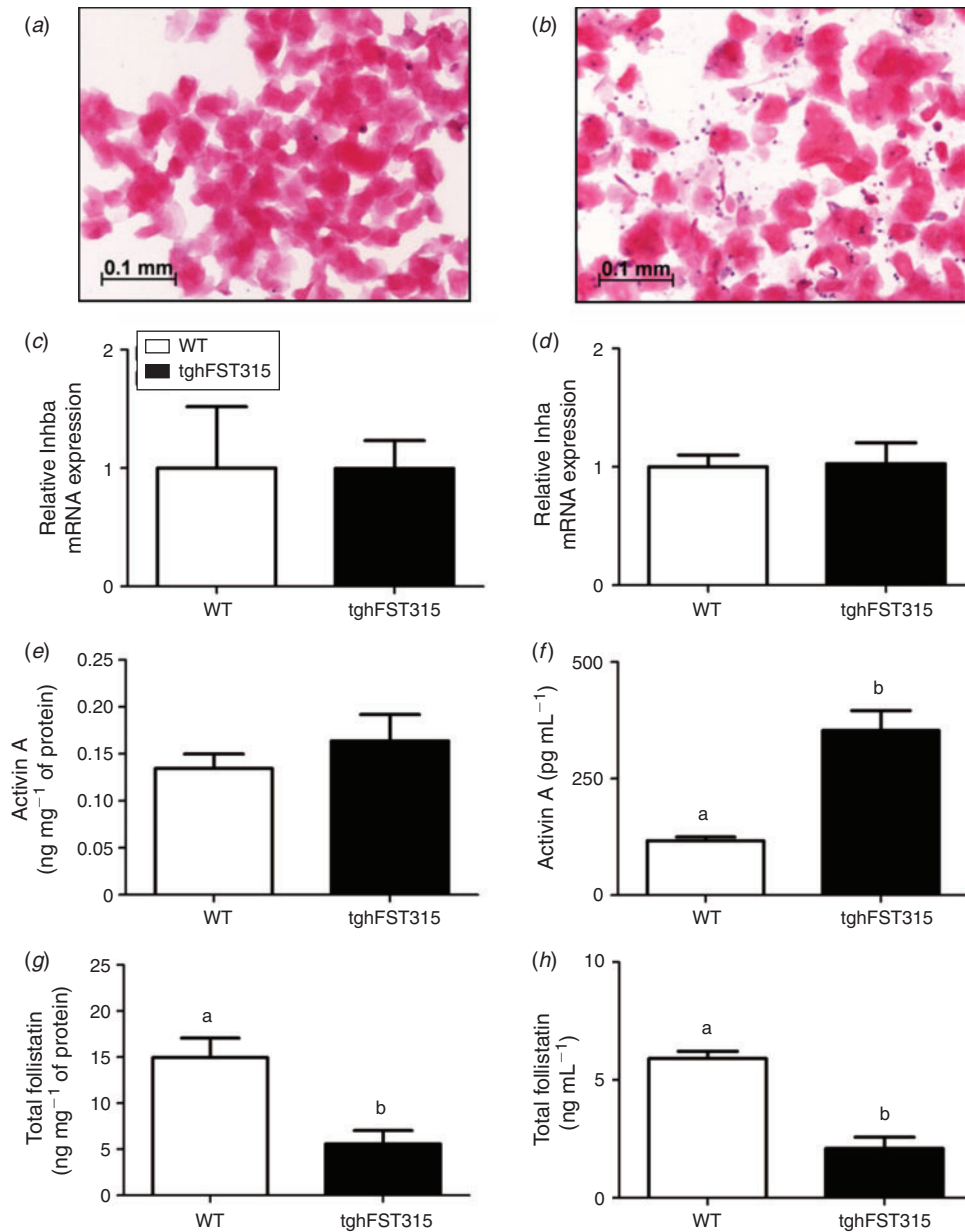


**Fig. 4.** Uterine and circulating levels of total FST and activin A are altered in tghFST315 mice. Representative micrographs of HandE-stained vaginal smears from (a) WT mouse at oestrus and a daily smear from (b) tghFST315 mouse. Scale bar is equal to 0.1 mm. Relative mRNA expression of (c) *Inhba* and (d) *Inha* from WT (at oestrus) and tghFST315 uteri. Protein expression of (e, f) activin A and (g, h) total FST for WT and tghFST315 mice. Graphs (e) and (g) represent expression of activin A and total FST from whole uterine tissue homogenates, displayed as ng of activin A or FST per mg of total protein. Graphs (f) and (h) represent expression of activin A and total FST from sera, displayed as ng mL<sup>-1</sup> or pg mL<sup>-1</sup>. Samples sizes were  $n = 3-6$  per genotype. Messenger RNA and protein data are displayed as mean  $\pm$  s.e.m. Data were compared by independent sample *t*-tests and bars that do not share a common letter are significantly different ( $P < 0.05$ ).

The tghFST315 genotype did not affect cell proliferation in glandular epithelium compared with WT mice (Fig. 6b). However, P treatment significantly reduced glandular epithelium proliferation in both WT and tghFST315 mice compared with vehicle and E-treated animals (vehicle:  $5.9 \pm 1.0\%$ ,

E:  $8.1 \pm 1.1\%$ , P:  $0.3 \pm 0.9\%$ ;  $F_{(2,27)} = 16.078$ ,  $P = < 0.001$ ; Fig. 6b). It is noted that gland numbers were reduced in tghFST315 mice and as a consequence, only  $n = 4-5$  mice were included in glandular epithelium proliferation counts per treatment group. The percentage of proliferating cells in the luminal

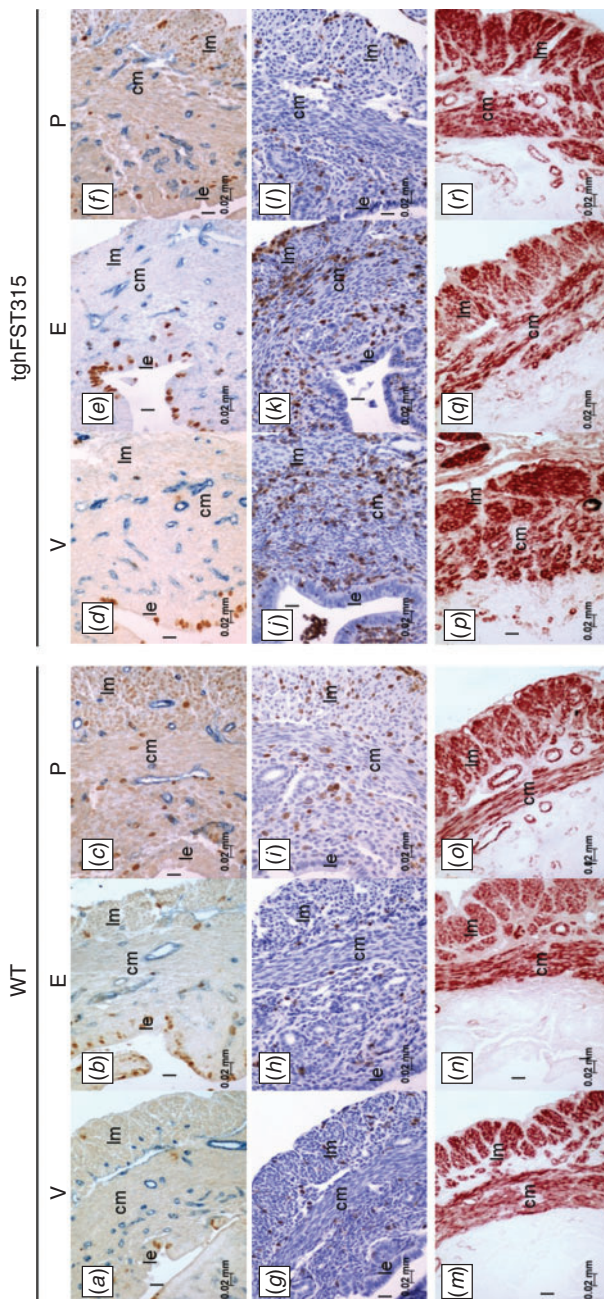


**Fig. 5.** Uterine immunostaining from ovariectomised tghFST315 and WT mice following exogenous E and P exposure. Representative micrographs of (a–f) BrdU (brown) and CD31 (blue), (g–l) CD45 and (m–r)  $\alpha$ SMA immunostaining from WT and tghFST315 mouse uteri following ovariectomy and subsequent treatment with vehicle (V), oestrogen (E) or progesterone (P). Samples sizes were  $n=7-9$  per genotype. Scale bar is equal to 0.02 mm. l, lumen; le, lumen epithelium; cm, circular myometrial layer; lm, longitudinal myometrial layer.

epithelium was significantly increased in E-treated mice (WT:  $43.1 \pm 4.8\%$ , tghFST315:  $25.8 \pm 6.1$ ) relative to vehicle (WT:  $8.5 \pm 2.0\%$ , tghFST315:  $8.9 \pm 2.7\%$ ) and P-treated animals (WT:  $0.7 \pm 0.5$ , tghFST315:  $3.5 \pm 2.3$ ;  $F_{(2,34)} = 43.154$ ,

$P < 0.001$ ). However, the increase in proliferation following E treatment was significantly reduced in tghFST315 mice relative to WT mice (Fig. 6c).

There was no significant effect of the tghFST315 genotype or hormone treatment on cell proliferation in the myometrium (Fig. 6d). However, there was a significant interaction term between genotype and hormone treatment ( $F_{(2,35)} = 4.613$ ,  $P = 0.017$ ; Fig. 6d). In the myometrium, the highest cell proliferation was seen following E treatment in tghFST315 mice compared with WT (WT:  $170.4 \pm 134.6$  cells  $\text{mm}^{-2}$ , tghFST315:  $851.4 \pm 134.6$  cells  $\text{mm}^{-2}$ ;  $P = 0.012$ ; Fig. 6d).

Endothelial cell proliferation was quantified in the endometrium and myometrium (Fig. 6e, f). Within endometrial vessels, endothelial cell proliferation in tghFST315 mice was not different from that in WT; however, there was an overall effect of hormone treatment ( $F_{(2,35)} = 14.750$ ,  $P < 0.001$ ), where E and P significantly increased endothelial cell proliferation (Fig. 6e). In the myometrium, both tghFST315 genotype ( $F_{(1,35)} = 6.170$ ,  $P = 0.018$ ) and hormone treatments ( $F_{(2,35)} = 7.870$ ,  $P = 0.002$ ) significantly influenced endothelial cell proliferation (Fig. 6f). However, unlike endometrial vessels, only E treatment increased proliferation of myometrial endothelial cells.

#### *Inflammation persisted in the uteri of tghFST315 mice following ovariectomy*

Following ovariectomy, leukocytes were still abundant in vehicle-treated tghFST315 uteri (Fig. 5j) compared with WT mice (Fig. 5g). Quantification confirmed that the abundance of CD45-positive cells in tghFST315 uteri was significantly increased compared with WT mice (WT:  $7.4 \pm 2.2\%$  positive cells, tghFST315:  $23.8 \pm 2.3\%$  positive cells;  $F_{(1,36)} = 27.620$ ,  $P < 0.001$ ; Fig. 7d). In the endometrium, tghFST315 genotype ( $F_{(1,36)} = 24.490$ ,  $P < 0.001$ ) and E treatment ( $F_{(2,36)} = 4.070$ ,  $P = 0.026$ ) significantly increased the percentage of CD45-positive leukocytes (Fig. 7e). In the myometrium, tghFST315 genotype ( $F_{(1,36)} = 25.900$ ,  $P < 0.001$ ) and E hormone treatment ( $F_{(2,36)} = 4.230$ ,  $P = 0.022$ ) also significantly increased leukocyte abundance (Fig. 7f). There was a significant interaction term between genotype and hormone regime ( $F_{(2,36)} = 4.030$ ,  $P = 0.026$ ). The tghFST315 mice also had greater abundance of CD45-positive cells in the luminal epithelium ( $F_{(1,35)} = 9.690$ ,  $P = 0.004$ ) and glandular epithelium ( $F_{(1,35)} = 6.496$ ,  $P = 0.016$ ; Fig. 7g, h).

E treatment significantly augmented the leukocyte response in tghFST315 endometrium and myometrium. In the E-treated tghFST315 endometrium, CD45-positive cells were increased compared with all WT groups (tghFST315 E:  $30.6 \pm 5.9\%$  positive cells, WT vehicle:  $6.9 \pm 1.5\%$  positive cells, WT E:  $8.4 \pm 3.8\%$  positive cells, WT P:  $3.6 \pm 1.0\%$  positive cells; Fig. 7e), whereas in the E-treated myometrium, leukocytes were significantly elevated in tghFST315 mice compared with all WT groups and tghFST315 vehicle and P-treated animals (tghFST315 E:  $34.2 \pm 7.3\%$  positive cells, WT vehicle:  $7.2 \pm 1.2\%$  positive cells, WT E:  $7.5 \pm 1.9\%$  positive cells, WT P:  $7.3 \pm 1.1\%$  positive cells, tghFST315 vehicle  $15.6 \pm 2.0\%$  positive cells, tghFST315 P:  $17.2 \pm 3.6\%$  positive cells; Fig. 7f).

Examination of  $\alpha$ SMA immunostaining revealed that the myometrial organisation of tghFST315 uteri did not improve

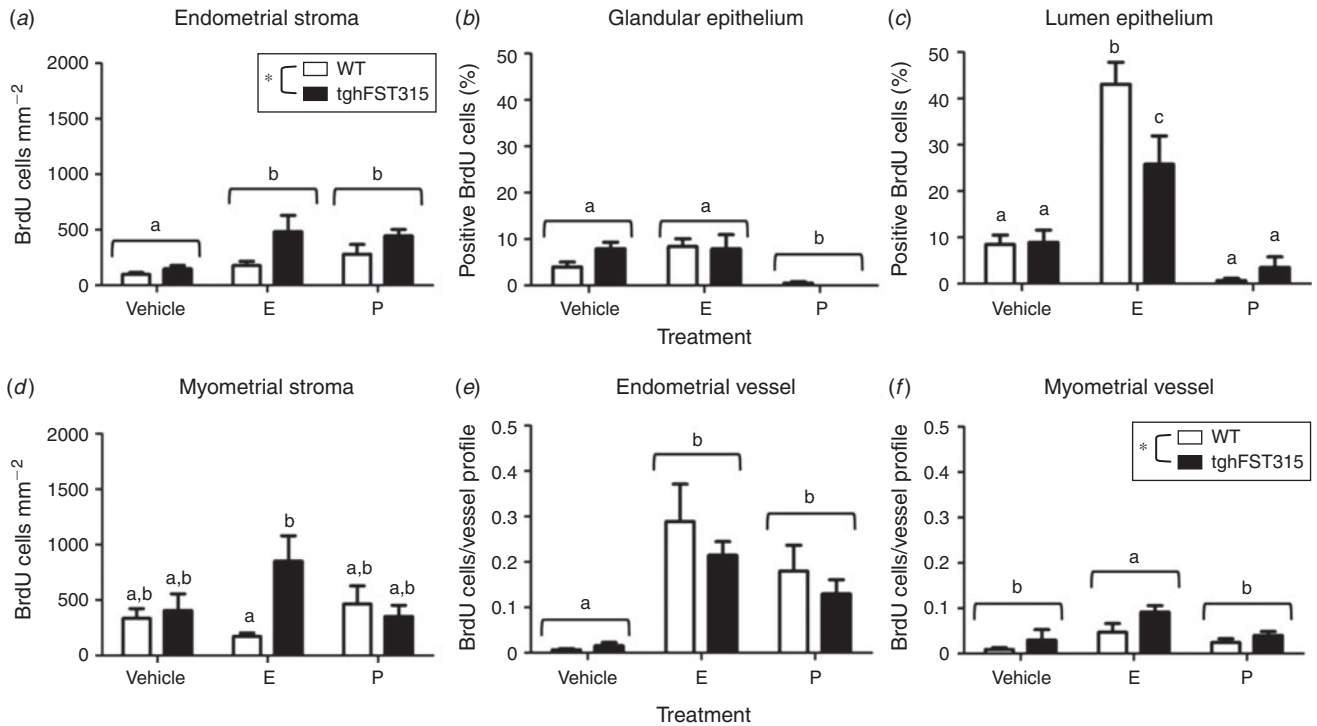


**Fig. 6.** Uterine cell proliferation in ovariectomised WT and tghFST315 mice following hormone treatment. BrdU proliferating cells (stained brown) were quantified as described in Materials and Methods. (a) Number of BrdU-positive cells per mm<sup>2</sup> in the endometrium, (b) percentage of BrdU-positive glandular epithelial cells (%), (c) percentage of BrdU-positive luminal epithelial cells (%), (d) number of BrdU-positive cells per mm<sup>2</sup> in the myometrium, (e) number of BrdU-positive cells per vessel profile in the endometrium and (f) number of BrdU-positive cells per vessel profile in the myometrium. Samples sizes were  $n = 6-9$  per genotype. Data are displayed as mean  $\pm$  s.e.m. Data were analysed by two-way ANOVA followed by Tukey's post-hoc tests. Significant differences between WT (white bars) and tghFST315 (black bars) genotypes are denoted by \* ( $P < 0.05$ ). Treatment groups that do not share a letter in common are significantly different ( $P < 0.05$ ). E, oestrogen; P, progesterone.

following ovariectomy (vehicles; Fig. 5m, p) or following treatment with E (Fig. 5n, q) or P (Fig. 5o, r). In Study 1, we observed that tghFST315 endometrium had reduced gland numbers compared with WT animals (Fig. 2e-h). In Study 3, quantification demonstrated that vehicle-treated WT mice ( $n = 15$ ) had significantly more endometrial gland profiles compared with vehicle-treated tghFST315 mice ( $n = 8$ ; WT:  $16.47 \pm 1.93$ , tghFST315:  $5.75 \pm 2.09$ ;  $P = < 0.000$ ; Fig. S4).

## Discussion

Our results demonstrate that FST is not required for embryonic development of the mouse oviduct and uterus (Müllerian duct). However, using transgenic mouse models we have shown that FST plays essential roles in the postnatal development of the uterus and oviduct. Adult transgenic mice expressing only FST315 (and completely lacking FST288) on a mouse FSTKO background had abnormal oviducts (failed coiling) and uterine horns, including abnormal myometrial smooth-muscle organisation and sustained leukocyte infiltration. As the FST315 isoform alone was insufficient to restore normal ovarian function (tghFST315 mice had decreased follicular pool, lack of corpora lutea and abnormal oestrous cycles; Lin *et al.* 2008), the reproductive tract abnormalities

may reflect abnormal ovarian function. However, the overt inflammation in the endometrium and myometrium of tghFST315 mice was maintained after ovariectomy and further exacerbated by administration of exogenous oestrogen. This raises the possibility that the abnormalities seen in tghFST315 mice may reflect a localised imbalance of FST and TGFB family members in the uterus itself, independent of the ovary. Our research highlights the need for further studies examining the interaction of ovarian versus uterine production of FST and TGFB family members in uterine development and function.

To date, there is very little information describing the role of FST in uterine development and function. Based on expression studies, there is evidence for a role for FST and activin A in embryonic development of the pelvis, gonads and urogenital septum (Feijen *et al.* 1994; Yao *et al.* 2004). However, there is no data that demonstrates a role for FST in the development of the Müllerian duct (oviduct, uterus, cervix and upper vagina). Our data do not support a role for FST in embryonic Müllerian tract development since PND0 tghFST315, tghFST288 and FSTKO mice all displayed normal oviduct and uterine gross anatomy and histology compared with WT pups. On the other hand, postnatal development of the oviducts and uterus were abnormal in tghFST315 mice. These abnormalities consisted of uteri that were oedematous and distended with areas of

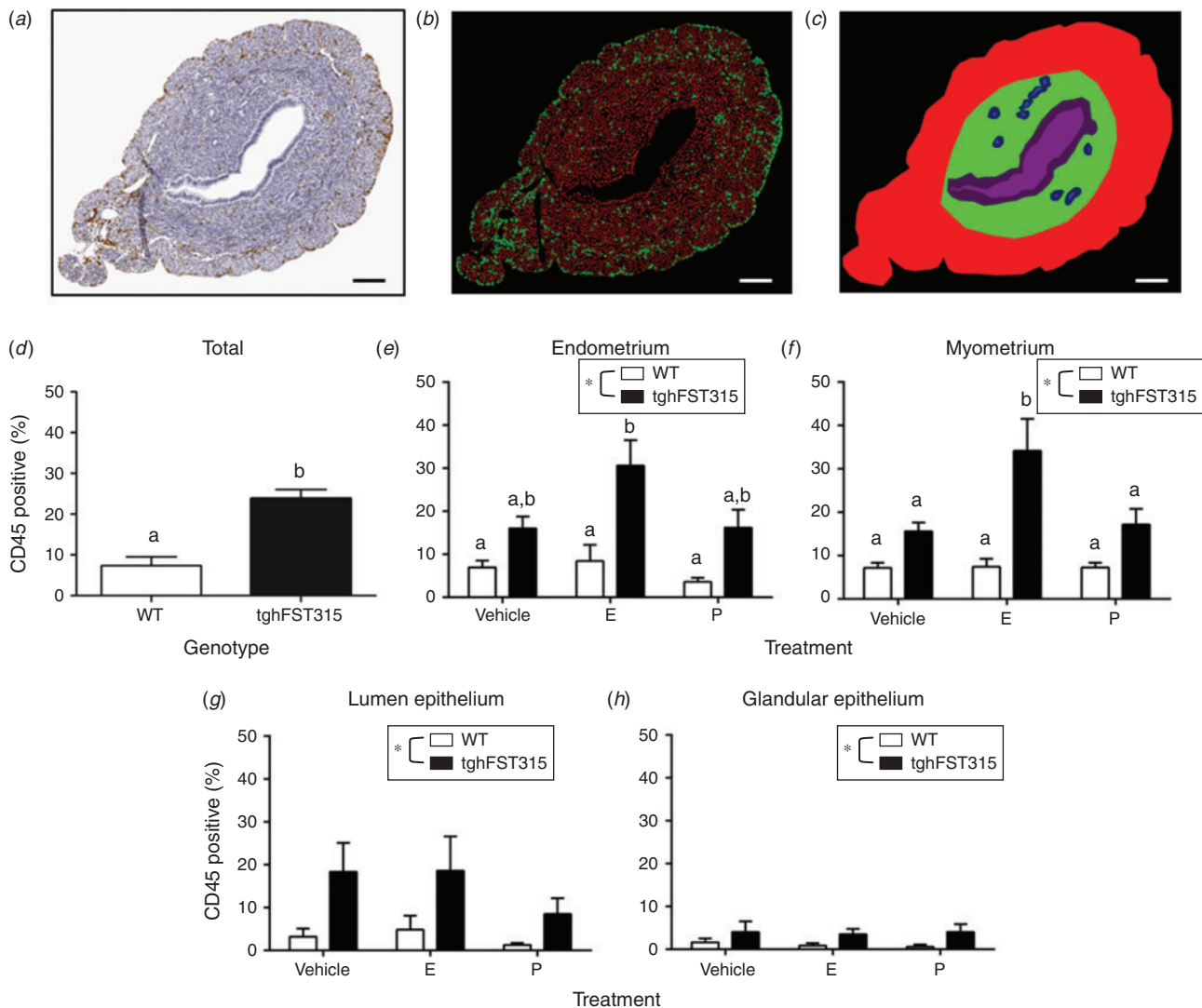


**Fig. 7.** TghFST315 genotype and E treatment increased uterine CD45 abundance. The effect of tghFST315 genotype and hormone treatment on CD45 abundance was quantified in ovariectomised mouse uteri as described in Materials and Methods. (a) Representative micrograph of a CD45-immunostained section used in image analysis. (b) The same image following colour deconvolution with green representing CD45-positive cells and red representing CD45-negative cells and (c) the same image divided into defined tissue regions; myometrial stroma in red, endometrial stroma in green, glandular epithelium in blue and lumen epithelium in purple. (d) Percentage of total CD45-positive cells in vehicle-treated uteri from WT and tghFST315 mice, (e) percentage of CD45-positive cells in the endometrial stroma, (f) percentage of CD45-positive cells in the myometrium, (g) percentage of CD45-positive cells in the luminal epithelium and (h) percentage of CD45-positive cells in the glandular epithelium. Samples sizes were  $n = 6-9$  per genotype. Data are displayed as mean  $\pm$  s.e.m. Data were analysed by two-way ANOVA followed by Tukey's post-hoc tests. Significant genotype differences are denoted by \* and groups that do not share a letter in common are also significantly different ( $P < 0.05$ ). E, oestrogen; P, progesterone.

constriction consistent with fibrosis and scarring. In adult tghFST315 mice there was evidence of disorganised muscle layers within the myometrium, and endometrial gland numbers were reduced. In addition, the oviducts of tghFST315 mice failed to coil. This later abnormality is not visible at PND0 as the coiling of the oviduct occurs in the first week after birth (Stewart and Behringer 2012). The lack of coiling in tghFST315 mice contrasts with observations in males lacking activin A due to the deletion of *Inhba* in the male reproductive tract, which leads to a loss of coiling in the epididymis

(Tomaszewski *et al.* 2007). Several genes control female reproductive tract and Müllerian duct development, in particular members of the *Wnt* and *Hox* families (reviewed by Massé *et al.* 2009). Evidence exists for a relationship between the FST and activin pathway and *Wnt4* and *Hoxa-10* regulation in the uteri of rodents (Katayama *et al.* 2006; Ciarmela *et al.* 2008). Future studies should explore these relationships further during the postnatal development, including during the pre-pubertal period, of the mouse reproductive tract. Therefore, postnatally, FST plays an important role in regulating the

integrity and maturation of the uterus (myometrium and adenogenesis) and coiling of the oviduct.

Several other studies related to activin A and FST also identify abnormalities of the oviduct and uterus. For example, mice overexpressing FST have abnormally thin and small uteri compared with WT animals (Guo *et al.* 1998). In sheep, high levels of FST expression during the critical period of coiling and branching of endometrial glands (PND 21–56) implicates a role for FST in postnatal adenogenesis (Hayashi *et al.* 2003). Similar to the oviducts and uteri of tghFST315 mice, conditional knock-outs of the TGFB Type 1 receptor in the female reproductive tract resulted in severely distorted oviducts (bilateral diverticula) consistent with defective smooth-muscle development in the myometrium and oviduct (Li *et al.* 2011).

The tghFST315 mouse is fundamentally a FST-deficient model. Although tghFST315 mice express human *FST315* on a mouse FSTKO background, total FST protein expression was reduced in the uteri and in serum compared WT animals (note that it is not currently possible to quantify FST protein at the isoform-specific level). It also remains unknown what effect the tghFST315 genotype has on *FST303* expression. Uterine activin A protein and *Inhba* mRNA were unchanged in tghFST315 mice; however, circulating activin A was elevated. Activin A is a key pro-inflammatory protein that predominantly acts early in the inflammatory cascade (acute phase) and also drives fibrosis (de Kretser *et al.* 1999; Hedger *et al.* 2011; de Kretser *et al.* 2012). For example, following a lipopolysaccharide (LPS) challenge in mice, pro-inflammatory cytokines and activin A rapidly increase in the serum (Jones *et al.* 2007). This response can be significantly attenuated by FST pretreatment (Jones *et al.* 2007). In contrast, activin A can be anti-inflammatory during chronic inflammation (reviewed by Hedger *et al.* 2011; de Kretser *et al.* 2012). The inflammation observed in tghFST315 mice is restricted to the reproductive tract and is not observed in other organs (Lin *et al.* 2008); this is a puzzling observation considering that activin A levels were increased systemically. While the exact mechanism for this tissue-specific effect is not understood, the FST-deficient uterus appears to be particularly vulnerable to the effects of inflammation. The inflammation of the oviduct and uterus in the tghFST315 mouse was chronic, but unlike classical chronic inflammatory responses, these mice are deficient in FST, thereby removing a major mechanism of neutralising the bioactivity and clearance of activin A. It is difficult to determine the source of circulating activin A protein due in part to the extensive number of tissues that express this protein, and secondly to the dimeric nature of the protein (reviewed by Hedger *et al.* 2011). However, bone marrow-derived neutrophils have been identified as an important source of activin A (Wu *et al.* 2012, 2013) and constituted a large proportion of the leukocyte infiltrate seen in the oviducts and uteri of adult tghFST315 mice.

We acknowledge that defective development of the oviducts and uteri in tghFST315 mice may directly reflect the abnormal ovarian phenotype of these animals (Lin *et al.* 2008). Early during the postnatal period development of the uterus is independent of the ovaries. However, between PND 10 and 26, uterine growth and development is ovarian-dependent (Branham and Sheehan 1995; Spencer *et al.* 2012). Since the

ovaries of tghFST315 mice are severely abnormal, maturing oviducts and uteri would not encounter the normal ovarian-dependent milieu required for normal development. Additionally, it is hypothesised that uterine function is programmed by developmental events that take place in the uterus during prenatal and postnatal maturation (reviewed by Spencer *et al.* 2012). We therefore surmise that in the absence of normal physiological levels of FST, the uteri of tghFST315 mice are already developmentally disadvantaged before reaching adulthood.

Ovarian hormones play a central role in controlling the influx of neutrophils and monocytes–macrophages into the uterus (Kachkache *et al.* 1991; Hunt 1994; Tibbetts *et al.* 1999). Surprisingly, following ovariectomy, tghFST315 mice maintained the overt inflammatory response in the uterus, which was exacerbated further by administration of oestrogen. Under normal circumstances, progesterone antagonises the effects of oestrogen on neutrophil migration to the uterus in a progesterone receptor (PR)-dependent manner (Tibbetts *et al.* 1999). Such a mechanism is in doubt in tghFST315 mice since they do not develop corpora lutea, and subsequently do not have the capacity to produce progesterone. In support, PRKO mice also show gross uterine inflammation and oedema (Lydon *et al.* 1996), similar to tghFST315 mice. Lydon *et al.* (1996) correlate their PRKO mice to an oestrogen-hypersensitive phenotype observed following long-term exposure to oestrogen. Therefore, a second possible mechanism responsible for the uterine-specific inflammation supports the hypothesis of Lin *et al.* (2008), where it was proposed that the inflammation seen in the tghFST315 uterus may reflect the inability of the tghFST315 mice to form corpora lutea, and therefore progesterone, resulting in an unopposed oestrogen environment (Lin *et al.* 2008). Further support for this view comes from the similar phenotypes observed in adult rats treated neonatally with oestrogen, which possess fewer uterine glands, have abnormal oestrous cycles and lack corpora lutea (Branham *et al.* 1985; Shiorta *et al.* 2012). However, a feature of the tghFST315 ovary was reduced follicle numbers (Lin *et al.* 2008), therefore oestradiol production may be poor and an alternative hypothesis must be considered. Premature cessation of mating behaviour in older female tghFST315 mice is consistent with premature cessation of oestradiol secretion by the ovaries (Lin *et al.* 2008). It is clear that additional research must address the interaction of ovarian hormones with uterine phenotype to address these apparently contradictory hypotheses.

This investigation has broadened the current understanding of FST in uterine biology; however, there were limitations to the study. Foremost, studies of the reproductive tract of tghFST315 females at pre-pubertal time points are required to precisely determine the timing of developmental abnormalities and interactions with ovarian hormones. We were unable to fully address the isoform-specific roles of FST288 and FST315 (and FST303) proteins due in part to the lack of commercially available isoform-specific FST antibodies and, secondly, due to our inability to study tghFST288 mice beyond PND0. Additional studies using the mutant mouse line expressing mouse FST288 only would be valuable (Kimura *et al.* 2010). Further, although tghFST315 mice survive to adulthood with complete reversal of the abnormal lung phenotype in the FSTKO (Lin *et al.* 2008),

the serum levels of FST are significantly lower than in WT mice. Therefore, future studies might benefit from conditional knock-out models.

This work has identified novel roles for FST in the development and function of the oviducts and uterus in mice and highlights the need for more detailed studies of FST and its interactions with other factors affecting the ontology of this system. Adult tghFST315 mice have grossly abnormal oviducts (including absent coiling) and uteri (disorganised myometrium and reduced gland numbers), secondary to poorly organised muscle layers and overt leukocyte infiltrate. We believe that these characteristics are, at least in part, intrinsic to the uterus and are not solely due to the influence of the abnormal ovary; however, additional studies to further define the specific ovarian and uterine effects are required. Further, while it is clear that the inflammatory response in the reproductive tract of tghFST315 mice is influenced by the steroid hormones oestrogen and progesterone, it is still unclear why the response is restricted to the reproductive tract. Further work is also necessary to explore isoform-specific roles of FST variants in reproductive tract function. However, this investigation demonstrates that in addition to its important ovarian roles, FST is also fundamental to the development and function of the oviduct and uterus.

### Acknowledgements

The authors wish to thank the staff of the Monash Medical Centre Animal House and Sarah Badelow, Matthew Chapman (Victorian Cancer Biobank, Royal Melbourne Hospital), Sue Haywood, Fiona Lederman, Michelle Lockhart, Carl Sprung, Yuqing Yang and Marina Zaitseva for their technical help and assistance. The research was supported by a National Health and Medical Research Council Project Grant (No. 606545) to J. E. G., M. P. H., D. M. deK. and P. A. W. R., the Victorian Government's Operational Infrastructure Support Program and a Monash Postgraduate Scholarship to R. G. C.

### References

- Branham, W. S., and Sheehan, D. M. (1995). Ovarian and adrenal contributions to postnatal growth and differentiation of the rat uterus. *Biol. Reprod.* **53**(4), 863–872. doi:10.1095/BIOLREPROD53.4.863
- Branham, W. S., Sheehan, D. M., Zehr, D. R., Ridlon, E., and Nelson, C. J. (1985). The postnatal ontogeny of rat uterine glands and age-related effects of 17 beta-oestradiol. *Endocrinology* **117**(5), 2229–2237. doi:10.1210/ENDO-117-5-2229
- Brody, J. R., and Cunha, G. R. (1989). Histologic, morphometric and immunocytochemical analysis of myometrial development in rats and mice. 1. Normal development. *Am. J. Anat.* **186**(1), 1–20. doi:10.1002/AJA.1001860102
- Ciarmela, P., Wiater, E., and Vale, W. (2008). Activin-A in myometrium: characterisation of the actions on myometrial cells. *Endocrinology* **149**(5), 2506–2516. doi:10.1210/EN.2007-0692
- Craythorn, R. G., Girling, J. E., Hedger, M. P., Rogers, P. A., and Winnall, W. R. (2009). An RNA-spiking method demonstrates that 18S rRNA is regulated by progesterone in the mouse uterus. *Mol. Hum. Reprod.* **15**(11), 757–761. doi:10.1093/MOLEHR/GAP058
- Craythorn, R. G., Winnall, W. R., Lederman, F., Gold, E. J., O'Connor, A. E., de Kretser, D. M., Hedger, M. P., Rogers, P. A., and Girling, J. E. (2012). Progesterone stimulates expression of follistatin splice variants Fst288 and Fst315 in the mouse uterus. *Reprod. Biomed. Online* **24**(3), 364–374. doi:10.1016/J.RBMO.2011.12.004
- de Kretser, D. M., Hedger, M. P., and Phillips, D. J. (1999). Activin A and follistatin: their role in the acute-phase reaction and inflammation. *J. Endocrinol.* **161**(2), 195–198. doi:10.1677/JOE.0.1610195
- de Kretser, D. M., O'Hehir, R. E., Hardy, C. L., and Hedger, M. P. (2012). The roles of activin A and its binding protein, follistatin, in inflammation and tissue repair. *Mol. Cell. Endocrinol.* **359**(1–2), 101–106. doi:10.1016/J.MCE.2011.10.009
- Feijen, A., Goumans, M. J., and van den Eijnden-van Raaij, A. J. (1994). Expression of activin subunits, activin receptors and follistatin in post-implantation mouse embryos suggests specific developmental functions for different activins. *Development* **120**(12), 3621–3637.
- Girling, J. E., Lederman, F. L., Walter, L. M., and Rogers, P. A. (2007). Progesterone, but not oestrogen, stimulates vessel maturation in the mouse endometrium. *Endocrinology* **148**(11), 5433–5441. doi:10.1210/EN.2007-0856
- Guo, Q., Kumar, T. R., Woodruff, T., Hadsell, L. A., DeMayo, F. J., and Matzuk, M. M. (1998). Overexpression of mouse follistatin causes reproductive defects in transgenic mice. *Mol. Endocrinol.* **12**(1), 96–106. doi:10.1210/MEND.12.1.0053
- Hashimoto, O., Nakamura, T., Shoji, H., Shimasaki, S., Hayashi, Y., and Sugino, H. (1997). A novel role of follistatin, an activin-binding protein, in the inhibition of activin action in rat pituitary cells. Endocytotic degradation of activin and its acceleration by follistatin associated with cell-surface heparan sulfate. *J. Biol. Chem.* **272**(21), 13 835–13 842. doi:10.1074/JBC.272.21.13835
- Hayashi, K., Carpenter, K. D., Gray, C. A., and Spencer, T. E. (2003). The activin–follistatin system in the neonatal ovine uterus. *Biol. Reprod.* **69**(3), 843–850. doi:10.1095/BIOLREPROD.103.016287
- Hedger, M. P., Winnall, W. R., Phillips, D. J., and de Kretser, D. M. (2011). The regulation and functions of activin and follistatin in inflammation and immunity. *Vitam. Horm.* **85**, 255–297. doi:10.1016/B978-0-12-385961-7.00013-5
- Heryanto, B., and Rogers, P. A. W. (2002). Regulation of endometrial endothelial cell proliferation by oestrogen and progesterone in the ovariectomised mouse. *Reproduction* **123**(1), 107–113. doi:10.1530/REP.0.1230107
- Hunt, J. S. (1994). Immunologically relevant cells in the uterus. *Biol. Reprod.* **50**(3), 461–466. doi:10.1095/BIOLREPROD50.3.461
- Jones, R. L., Salamonsen, L. A., and Findlay, J. K. (2002a). Activin A promotes human endometrial stromal cell decidualisation *in vitro*. *J. Clin. Endocrinol. Metab.* **87**(8), 4001–4004. doi:10.1210/JCEM.87.8.8880
- Jones, R. L., Salamonsen, L. A., and Findlay, J. K. (2002b). Potential roles for endometrial inhibins, activins and follistatin during human embryo implantation and early pregnancy. *Trends Endocrinol. Metab.* **13**(4), 144–150. doi:10.1016/S1043-2760(01)00559-8
- Jones, K. L., Mansell, A., Patella, S., Scott, B. J., Hedger, M. P., de Kretser, D. M., and Phillips, D. J. (2007). Activin A is a critical component of the inflammatory response, and its binding protein, follistatin, reduces mortality in endotoxemia. *Proc. Natl. Acad. Sci. USA* **104**(41), 16 239–16 244. doi:10.1073/PNAS.0705971104
- Jorgez, C. J., Klysik, M., Jamin, S. P., Behringer, R. R., and Matzuk, M. M. (2004). Granulosa cell-specific inactivation of follistatin causes female fertility defects. *Mol. Endocrinol.* **18**(4), 953–967. doi:10.1210/ME.2003-0301
- Kachkache, M., Acker, G. M., Chaouat, G., Noun, A., and Garabedian, M. (1991). Hormonal and local factors control the immunohistochemical distribution of immunocytes in the rat uterus before conceptus implantation – effects of ovariectomy, fallopian-tube section and injection. *Biol. Reprod.* **45**(6), 860–868. doi:10.1095/BIOLREPROD45.6.860
- Katayama, S., Ashizawa, K., Fukuhara, T., Hiroyasu, M., Tsuzuki, Y., Tatamoto, H., Nakada, T., and Nagai, K. (2006). Differential expression patterns of Wnt and  $\beta$ -Catenin/TCF target genes in the uterus of immature female rats exposed to 17 $\alpha$ -ethynyl oestradiol. *Toxicol. Sci.* **91**(2), 419–430. doi:10.1093/TOXSCI/KFJ167

- Kimura, F., Sidis, Y., Bonomi, L., Xia, Y., and Schneyer, A. (2010). The follistatin-288 isoform alone is sufficient for survival but not for normal fertility in mice. *Endocrinology* **151**(3), 1310–1319. doi:10.1210/EN.2009-1176
- Knight, P. G., Satchell, L., and Glistler, C. (2012). Intra-ovarian roles of activins and inhibins. *Mol. Cell. Endocrinol.* **359**(1–2), 53–65. doi:10.1016/J.MCE.2011.04.024
- Lerch, T. F., Shimasaki, S., Woodruff, T. K., and Jardetzky, T. S. (2007). Structural and biophysical coupling of heparin and activin binding to follistatin isoform functions. *J. Biol. Chem.* **282**(21), 15930–15939. doi:10.1074/JBC.M700737200
- Li, Q., Agno, J. E., Edson, M. A., Nagaraja, A. K., Nagashima, T., and Matzuk, M. M. (2011). Transforming growth factor  $\beta$  receptor type 1 is essential for female reproductive tract integrity and function. *PLoS Genet.* **7**(10), e1002320. doi:10.1371/JOURNAL.PGEN.1002320
- Lin, S. Y., Craythorn, R. G., O'Connor, A. E., Matzuk, M. M., Girling, J. E., Morrison, J. R., and de Kretser, D. M. (2008). Female infertility and disrupted angiogenesis are actions of specific follistatin isoforms. *Mol. Endocrinol.* **22**(2), 415–429. doi:10.1210/ME.2006-0529
- Lydon, J. P., DeMayo, F. J., Conneely, O. M., and O'Malley, B. W. (1996). Reproductive phenotypes of the progesterone receptor null mutant mouse. *The Journal of Steroid Biochemistry and Molecular Biology* **56**(1–6), 67–77. doi:10.1016/0960-0760(95)00254-5
- Marcondes, F. K., Bianchi, F. J., and Tanno, A. P. (2002). Determination of the oestrous cycle phases of rats: some helpful considerations. *Braz. J. Biol.* **62**(4A), 609–614. doi:10.1590/S1519-69842002000400008
- Massé, J., Watrin, T., Laurent, A., Deschamps, S., Guerrier, D., and Pellerin, I. (2009). The developing female genital tract: from genetics to epigenetics. *Int. J. Dev. Biol.* **53**, 411–424. doi:10.1387/IJDB.082680JM
- Matzuk, M. M., Lu, N., Vogel, H., Sellheyer, K., Roop, D. R., and Bradley, A. (1995). Multiple defects and perinatal death in mice deficient in follistatin. *Nature* **374**(6520), 360–363. doi:10.1038/374360A0
- Mercado, M., Shimasaki, S., Ling, N., and DePaolo, L. (1993). Effects of oestrous cycle stage and pregnancy on follistatin gene expression and immunoreactivity in rat reproductive tissues: progesterone is implicated in regulating uterine gene expression. *Endocrinology* **132**(4), 1774–1781.
- Nakamura, T., Takio, K., Eto, Y., Shibai, H., Titani, K., and Sugino, H. (1990). Activin-binding protein from rat ovary is follistatin. *Science* **247**(4944), 836–838. doi:10.1126/SCIENCE.2106159
- O'Connor, A. E., McFarlane, J. R., Hayward, S., Yokhaichiya, T., Groome, N. P., and de Kretser, D. M. (1999). Serum activin A and follistatin concentrations during human pregnancy: a cross-sectional and longitudinal study. *Hum. Reprod.* **14**(3), 827–832. doi:10.1093/HUMREP/14.3.827
- Patel, K. (1998). Follistatin. *Int. J. Biochem. Cell Biol.* **30**(10), 1087–1093. doi:10.1016/S1357-2725(98)00064-8
- Petraglia, F., Gallinelli, A., Grande, A., Florio, P., Ferrari, S., Genazzani, A. R., Ling, N., and DePaolo, L. V. (1994). Local production and action of follistatin in human placenta. *J. Clin. Endocrinol. Metab.* **78**(1), 205–210.
- Pfaffl, M. W. (2001). A new mathematical model for relative quantification in real-time RT-PCR. *Nucleic Acids Res.* **29**(9), e45. doi:10.1093/NAR/29.9.E45
- Refaat, B., and Ledger, W. (2011). The expression of activins, their type II receptors and follistatin in human Fallopian tube during the menstrual cycle and in pseudo-pregnancy. *Hum. Reprod.* **26**(12), 3346–3354. doi:10.1093/HUMREP/DER331
- Schindelin, J., Arganda-Carreras, I., Frise, E., Kaynig, V., Longair, M., Pietzsch, T., Preibisch, S., Rueden, C., Saalfeld, S., Schmid, B., Tinevez, J. Y., White, D. J., Hartenstein, V., Eliceiri, K., Tomancak, P., and Cardona, A. (2012). Fiji: an open-source platform for biological-image analysis. *Nat. Methods* **9**(7), 676–682. doi:10.1038/NMETH.2019
- Shiorta, M., Kawashima, J., Nakamura, T., Ogawa, Y., Kamiie, J., Yasuno, K., Shirota, K., and Yoshida, M. (2012). Delayed effects of single neonatal subcutaneous exposure of low-dose 17 $\alpha$ -ethynylestradiol on reproductive function in female rats. *J. Toxicol. Sci.* **37**(4), 681–690. doi:10.2131/JTS.37.681
- Spencer, T. E., Dunlap, K. A., and Filant, J. (2012). Comparative developmental biology of the uterus: insights into mechanisms and developmental disruption. *Mol. Cell. Endocrinol.* **354**(1–2), 34–53. doi:10.1016/J.MCE.2011.09.035
- Stewart, C. A., and Behringer, R. R. (2012) Mouse oviduct development. In 'Mouse Development, Results and Problems in Cell Differentiation. Vol. 55'. (Ed. J. Z. Kubiak) pp. 247–262. (Springer-Verlag: Berlin Heidelberg.)
- Sugino, K., Kurosawa, N., Nakamura, T., Takio, K., Shimasaki, S., Ling, N., Titani, K., and Sugino, H. (1993). Molecular heterogeneity of follistatin, an activin-binding protein. Higher affinity of the carboxyl-terminal truncated forms for heparan sulfate proteoglycans on the ovarian granulosa cell. *J. Biol. Chem.* **268**(21), 15579–15587.
- Tibbetts, T. A., Conneely, O. M., and O'Malley, B. W. (1999). Progesterone via its receptor antagonises the pro-inflammatory activity of oestrogen in the mouse uterus. *Biol. Reprod.* **60**(5), 1158–1165. doi:10.1095/BIOLREPROD60.5.1158
- Tierney, E. P., and Giudice, L. C. (2004). Role of activin A as a mediator of *in vitro* endometrial stromal cell decidualisation via the cyclic adenosine monophosphate pathway. *Fertil. Steril.* **81**(Suppl. 1), 899–903.
- Tomaszewski, J., Joseph, A., Archambeault, D., and Yao, H. H.-C. (2007). Essential roles of inhibin beta A in mouse epididymal coiling. *Proc. Natl. Acad. Sci. USA* **104**(27), 11322–11327. doi:10.1073/PNAS.0703445104
- Walter, L. M., Rogers, P. A. W., and Girling, J. E. (2005). The role of progesterone in endometrial angiogenesis in pregnant and ovariectomised mice. *Reproduction* **129**(6), 765–777. doi:10.1530/REP.1.00625
- Walter, L. M., Rogers, P. A. W., and Girling, J. E. (2010). Vascular endothelial growth factor-A isoform and (co)receptor expression are differentially regulated by 17 $\beta$ -oestradiol in the ovariectomised mouse uterus. *Reproduction* **140**(2), 331–341. doi:10.1530/REP-10-0047
- Wankell, M., Munz, B., Hubner, G., Hans, W., Wolf, E., Goppelt, A., and Werner, S. (2001). Impaired wound healing in transgenic mice over-expressing the activin antagonist follistatin in the epidermis. *EMBO J.* **20**(19), 5361–5372. doi:10.1093/EMBOJ/20.19.5361
- Winnall, W. R., Muir, J. A., Liew, S., Hirst, J. J., Meachem, S. J., and Hedger, M. P. (2009). Effects of chronic celecoxib on testicular function in normal and lipopolysaccharide-treated rats. *Int. J. Androl.* **32**(5), 542–555. doi:10.1111/J.1365-2605.2008.00895.X
- Winnall, W. R., Muir, J. A., and Hedger, M. P. (2011). Rat resident testicular macrophages have an alternatively activated phenotype and constitutively produce interleukin-10 *in vitro*. *J. Leukoc. Biol.* **90**(1), 133–143. doi:10.1189/JLB.1010557
- Wu, H., Chen, Y., Winnall, W. R., Phillips, D. J., and Hedger, M. P. (2012). Acute regulation of activin A and its binding protein, follistatin, in serum and tissues following lipopolysaccharide treatment of adult male mice. *Am. J. Physiol. Regul. Integr. Comp. Physiol.* **303**(6), R665–R675. doi:10.1152/AJPREGU.00478.2011
- Wu, H., Chen, Y., Winnall, W. R., Phillips, D. J., and Hedger, M. P. (2013). Regulation of activin A release from murine bone marrow-derived neutrophil precursors by tumour necrosis factor- $\alpha$  and insulin. *Cytokine* **61**(1), 199–204. doi:10.1016/J.CYTO.2012.09.018
- Yao, H. H., Matzuk, M. M., Jorgez, C. J., Menke, D. B., Page, D. C., Swain, A., and Capel, B. (2004). Follistatin operates downstream of Wnt4 in mammalian ovary organogenesis. *Dev. Dyn.* **230**(2), 210–215. doi:10.1002/DVDY.20042